



An optical anion chemosensor based on a europium complex and its molecular logic behavior

Lianlian Wang^{a,b}, Bin Li^{a,*}, Liming Zhang^a, Peng Li^{a,b}, Hong Jiang^{a,*}

^aState Key Laboratory of Luminescence and Applications, Changchun Institute of Optics Fine Mechanics and Physics, Chinese Academy of Sciences, Changchun 130033, PR China

^bGraduate School of the Chinese Academy of Sciences, Chinese Academy of Sciences, Beijing 100039, PR China

ARTICLE INFO

Article history:

Received 27 August 2012

Received in revised form

16 October 2012

Accepted 22 November 2012

Available online 29 November 2012

Keywords:

Europium complex

AcO⁻ ion

Optical sensor

Oxygen

Energy backtransfer

Logic gate

ABSTRACT

In this paper, synthesis and photophysical properties of an organoeuropium complex, Eu(DBM)₃DPPZ (DBM = dibenzoylmethane, DPPZ = dipyrido [3,2-a:2',3'-c]phenazine), are described and discussed. The europium complex sensor can efficiently recognize AcO⁻ ion over other anions by the increase of luminescence intensity, which is applicable to naked eye detection for AcO⁻ ion. The sensing mechanism is ascribed to the replacement of DPPZ by AcO⁻ ion. Moreover, the Eu³⁺ emission is also found to be sensitive to molecular oxygen through a back-energy transfer mechanism. Based on these characters, this "off-on"-type luminescent sensor could successfully mimic an IMP (IMPLICATION) gate at molecular level with AcO⁻ ion and oxygen as inputs. The output of a sharp characteristic Eu³⁺ emission is read as "0" only in the absence of AcO⁻ ion under oxygen atmosphere. As far as we know, this is the first example of a logic gate corresponding to a two-input IMP function obtained from a europium complex.

© 2012 Elsevier Ltd. All rights reserved.

1. Introduction

Anions play fundamental roles in biological, security and environmental science [1] and thus have attracted considerable interests for their detection. Several approaches aiming at selective optical indicators for anions (such as F⁻ or AcO⁻), which provide extraordinary signal changes in absorption or luminescence spectra, have been presented in recent decades [2–9]. Among these numerous indicators, organic lanthanide complexes have been proved to be excellent candidates owing to their advantageous photophysical properties such as large Stokes shift, narrow emission bands and long excited state lifetimes [10–14]. Furthermore, the emission color depends only on the lanthanide ion and is independent of the environment of a given lanthanide ion. Among the lanthanides of interest, those enabling a simple and sensitive fluorimetric detection, such as Eu³⁺ and Tb³⁺, are particularly relevant [15–18].

It has been known for some time that counter ions can coordinate to lanthanide ions in coordinating unsaturated ligands to fulfill the coordination requirements of the lanthanides ions. Furthermore, it is also known that weakly-coordinated ligands can be

displaced by stronger ones [14]. Generally, there are two ways of modulating the emission property of lanthanide complexes by anions. Firstly, water molecules bound to the lanthanide center could be displaced by anions, leading to enhanced luminescent intensity; the other one is the displacement of ligands by anions resulting in the increase or decrease of luminescent intensity [4]. Li and coworkers [16] have nicely demonstrated a terbium complex for detecting anions by luminescence modulation through back-energy transfer mechanism. Upon addition of F⁻ ion, the terbium emission greatly increased and this change became saturated when F⁻ reached about three equivalents of the terbium complex. However, further addition of a large excess of F⁻ ion caused emission decrease. Similar emission modulation behavior of the terbium complex was also observed for AcO⁻ ion.

Besides being used as chemosensors for detecting anions, lanthanide complexes can also be applied in sensing other analytes, such as cations and oxygen, as well as mimicking a molecular level logic gate [19–24]. Optical oxygen sensors based on [Eu(TTA)₃(-phencarz)]/PS composite nanofibrous membranes were prepared in our previous work [20]. Gunnlaugsson and coworkers [22,23] reported terbium macrocyclic quinolyl conjugates as luminescent molecular switches and logic gate functions using H⁺/OH⁻ and O₂ as inputs. Pischel and coworkers [24] designed a molecular logic gate based on phthamide-sensitized Tb³⁺ luminescence with Cl⁻, O₂, and triethylamine as inputs. However, to the best of our knowledge, no

* Corresponding authors. Tel./fax: +86 431 86176935.

E-mail address: lib020@yahoo.cn (B. Li).

molecule logic device based on europium complexes has been reported although they have similar remarkable luminescent property as well as terbium complexes.

On the basis of the above opinions, we attempt to develop a luminescence probe based on an organic europium complex of $\text{Eu}(\text{DBM})_3\text{DPPZ}$ (DBM = dibenzoylmethane, DPPZ = dipyrido[3,2-a:2',3'-c]phenazine) [25], which could be applicable to detect AcO^- with naked eyes. Moreover, the Eu^{3+} emission is also found to be sensitive to molecular oxygen. According to these properties, a molecular level IMP (IMPLICATION) gate based on this “off–on”-type luminescence sensor could be successfully mimicked with AcO^- and oxygen as the two inputs where the output, a sharp characteristic Eu^{3+} emission, is read as “0” only in the absence AcO^- under oxygen atmosphere.

2. Experimental details

2.1. Materials and reagents

DBM and Eu_2O_3 (99.99%) were purchased from Aldrich Chemical Company and Sinopharm Chemical Reagent Company. $\text{EuCl}_3 \cdot 6\text{H}_2\text{O}$ was prepared by dissolving Eu_2O_3 in concentrated hydrochloric acid. All reagents and chemicals were used without further purification.

2.2. Instruments and methods

^1H NMR spectra were recorded using a mercury-300BB spectrometer (Varian, USA) operated at 300 MHz with tetramethylsilane (TMS) as internal standard. Elemental analyses were performed on a Carlo Erba 1106 elemental analyzer. The UV/Visible (UV/Vis) absorption spectra were obtained on a Shi-madzu-UV-3101 scanning spectrophotometer. Fluorescence spectra were measured with a Hitachi F-4500 fluorescence spectrophotometer with the excitation and the emission wavelength bandpasses were set at 2.5 nm and 1.0 nm, respectively. The luminescence lifetimes were obtained with 355 nm light generated from a third-harmonic-generator pump, using a pulsed Nd:YAG laser as the excitation source. The Nd:YAG laser possesses a line width of 1.0 cm^{-1} , a pulse duration of 10 ns, and a repetition frequency of 10 Hz. The quantum yield was measured by comparing fluorescence intensity (integrated areas) of a standard sample (Rhodamine 6G) and the unknown sample according to the following equation:

$$\Phi_{\text{unk}} = \frac{n_{\text{unk}}^2 A_{\text{ref}} I_{\text{unk}}}{n_{\text{ref}}^2 A_{\text{unk}} I_{\text{ref}}} \Phi_{\text{ref}} \quad (1)$$

where Φ_{unk} is the luminescence quantum yield of sample; $\Phi_{\text{ref}} = 0.92$ is the luminescence quantum yield of Rhodamine 6G (ethanol, 10^{-6} M) [16], I_{unk} and I_{ref} are the integrated fluorescence intensities of unknown sample and Rhodamine 6G, respectively; A_{unk} and A_{ref} are the absorbance of unknown sample and Rhodamine 6G at the wavelength of excitation. n_{unk} and n_{ref} are the refractive indexes of corresponding solvents (pure solvents were assumed). All spectrophotometric spectra were carried out in CH_3CN solutions at room temperature. For the sensitivity experiment toward dissolved oxygen, the solvent was bubbled by N_2 and O_2 alternately for ca. 20 min. with a degassing device.

2.3. Synthesis of $\text{Eu}(\text{DBM})_3\text{DPPZ}$

DPPZ was synthesized according to our previously reported procedure [26]. DPPZ: ^1H NMR (300 Hz, CDCl_3): δ (ppm) 9.65 (d, $J = 8.1\text{ Hz}$, 2H), 9.28 (d, $J = 3.3\text{ Hz}$, 2H), 8.37 (dd, $J = 6.6\text{ Hz}$, 6.3 Hz,

2H), 7.94 (dd, $J = 6.3\text{ Hz}$, 6.6 Hz, 2H), 7.82 (dd, $J = 8.1\text{ Hz}$, 8.1 Hz, 2H). $\text{Eu}(\text{DBM})_3\text{DPPZ}$ (Scheme 1) was obtained according to the conventional method with minor modifications as follows. DBM (0.067 g, 0.3 mmol) and DPPZ (0.028 g, 0.1 mmol) were dissolved in ethanol (10 mL) under stirring. Sodium hydroxide was added until the pH value of the solution approached 7. Then $\text{EuCl}_3 \cdot 6\text{H}_2\text{O}$ (0.037 g, 0.1 mmol) in water (2 mL) was added to the mixture solution. The mixture was stirred for 12 h under reflux. The product was collected by filtration and recrystallized from ethanol. Elemental analysis (%) calcd for $\text{C}_{63}\text{H}_{46}\text{EuN}_4\text{O}_6$: C, 68.35; H, 4.19; N, 5.06. Found: C, 68.11; H, 4.06; N, 5.17.

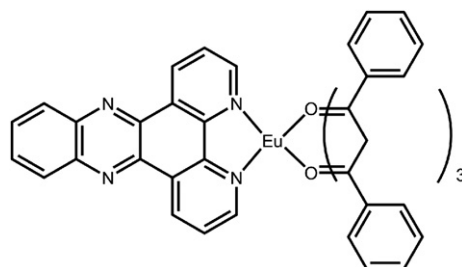
3. Results and discussion

3.1. Photophysical property of $\text{Eu}(\text{DBM})_3\text{DPPZ}$

Fig. 1 shows the UV–Vis absorption spectra of $\text{Eu}(\text{DBM})_3\text{DPPZ}$ (5 μM) and the free ligands (5 μM) in CH_3CN solutions, as well as the photoluminescence (PL) spectrum of the europium complex. The absorption maximum of free DBM at 348 nm is attributed to the $\pi-\pi^*$ enol absorption of the β -diketonate [27]. The $\pi-\pi^*$ electronic absorption of ligand DPPZ are located at 270 nm, 359 nm, and 375 nm [28]. As for $\text{Eu}(\text{DBM})_3\text{DPPZ}$, the absorption are located at 266 nm and 353 nm. It is observed that a red shift of the major $\pi-\pi^*$ electronic transition occurs compared with the absorption spectrum of free DBM and a blue shift after further coordinating with DPPZ, which may be attributed to the coordinative interactions between Eu^{3+} ion and the ligands. The sharp characteristic emission at 610 nm of the Eu^{3+} ion from $^5\text{D}_0-^7\text{F}_2$ transition is observed, accompanied by the weak emissions corresponding to $^5\text{D}_0-^7\text{F}_j$ ($J = 0, 1, 3, 4$) transitions as shown in Fig. 1. In addition, a weak emission band at $\sim 415\text{ nm}$, which attributes to the emission from DPPZ ligand, is also observed in the CH_3CN solution. This observation suggests that the excited state energy of DPPZ is not completely transferred to the emissive center, which will be later discussed.

To further investigate the luminescence property of $\text{Eu}(\text{DBM})_3\text{DPPZ}$, we selectively determined the emission quantum efficiencies and the lifetimes of the $^5\text{D}_0$ excited state for $\text{Eu}(\text{DBM})_3\text{DPPZ}$ and a reference complex of $\text{Eu}(\text{DBM})_3(\text{H}_2\text{O})_2$. As shown in Table 1, the quantum yield and the lifetime of $\text{Eu}(\text{DBM})_3\text{DPPZ}$ is 0.65% and 53 μs , respectively, which are greatly lower than those of $\text{Eu}(\text{DBM})_3(\text{H}_2\text{O})_2$, revealing that introducing DPPZ as the second ligand actually reduces the quantum yield and shortens the lifetime of Eu^{3+} ion. In fact, the lifetime is dominated by total radiative transition rate k_{rad} and nonradiative decay rate k_{nr} , which can be written as

$$\tau = \frac{1}{k_{\text{rad}} + k_{\text{nr}}} \quad (2)$$



Scheme 1. Molecular structure of $\text{Eu}(\text{DBM})_3\text{DPPZ}$.

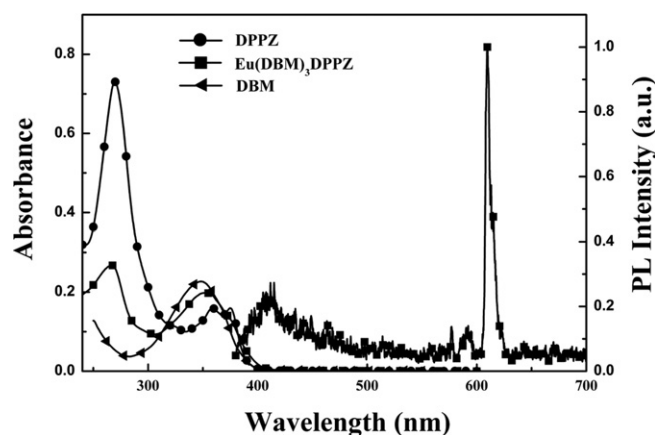


Fig. 1. Absorption and PL spectra of $\text{Eu}(\text{DBM})_3\text{DPPZ}$ ($5 \mu\text{M}$) and absorption spectra of the ligands ($5 \mu\text{M}$) in CH_3CN solutions.

$$\tau = \frac{\Phi}{k_{\text{rad}}} \quad (3)$$

The corresponding radiative and nonradiative decay rates are calculated and summarized in Table 1. It is found that the radiative transition rate of $\text{Eu}(\text{DBM})_3\text{DPPZ}$ is lower than that of $\text{Eu}(\text{DBM})_3(\text{H}_2\text{O})_2$.

The luminescence property of $\text{Eu}(\text{DBM})_3\text{DPPZ}$ could be explained by the energy transfer between ligands and central metal ion [20,27]. Generally, sensitization pathway in luminescent Eu^{3+} complexes consists of an initial strong absorption of UV energy that excites the ligands to excited S_1 and subsequent intersystem crossing of the ligands to their T_1 states. Finally, the energy is nonradiatively transferred to a resonance state of coordinated Eu^{3+} ion, which in turn, undergoes a multiphoton relaxation and subsequent emission in visible region. The singlet-state energy levels of DPPZ and DBM are estimated by referencing their absorption edges, which are calculated to be 3.10 eV (400 nm) and 3.07 eV (405 nm), respectively. The singlet- and triplet-state energy levels are illustrated in Fig. 2. The energy gaps ΔE ($^1\pi\pi^* \rightarrow ^3\pi\pi^*$) between $^1\pi\pi^*$ and $^3\pi\pi^*$ levels are 6533 and 5404 cm^{-1} for DPPZ and DBM, respectively, which shows that the intersystem crossing processes are effective for the two ligands [29]. The triplet energy levels of DPPZ and DBM are 2.29 eV (540 nm) and 2.4 eV (517 nm), respectively, as reported in our before works [27,30]. For $\text{Eu}(\text{DBM})_3\text{DPPZ}$, since the energy gap between $\text{Eu}^{3+} \ ^5\text{D}_0$ level ($17,500 \text{ cm}^{-1}$) [29] and the triplet energy of DPPZ is about 970 cm^{-1} , which is less than the critical value of 1500 cm^{-1} , the thermally activated energy backtransfer could occur [3], resulting the decrease of quantum efficiency and lifetime, as well as above mentioned inefficient energy transfer from excited state DPPZ to the emissive center.

3.2. PL spectral responses of $\text{Eu}(\text{DBM})_3\text{DPPZ}$ toward anions

In order to evaluate the sensitivity of the europium complex toward anions, PL spectral response profiles at 610 nm of the complex ($5 \mu\text{M}$) with different anions are recorded in CH_3CN

Table 1
Photophysical parameters for $\text{Eu}(\text{DBM})_3(\text{H}_2\text{O})_2$ and $\text{Eu}(\text{DBM})_3\text{DPPZ}$.

Complex	Abs. (nm)	Ex. (nm)	Em. (nm)	τ (μs)	Φ (%)	k_{rad} (s^{-1})	k_{nr} (s^{-1})
$\text{Eu}(\text{DBM})_3(\text{H}_2\text{O})_2$	352	357	610	175	4.73	270	5.43×10^3
$\text{Eu}(\text{DBM})_3\text{DPPZ}$	266, 353	364	610	53	0.65	123	1.87×10^4

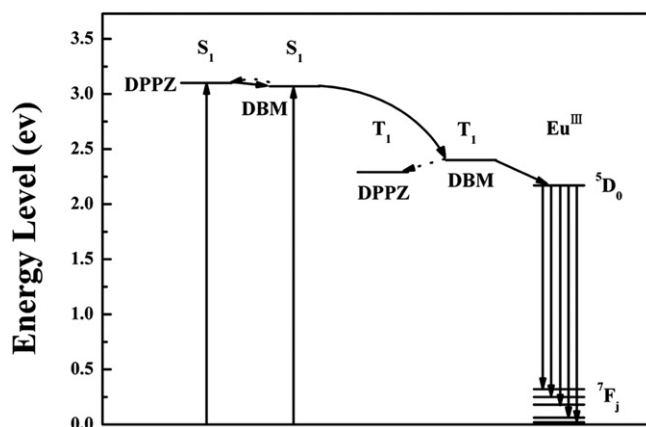


Fig. 2. Schematic energy-level diagram and energy-transfer process. S_1 : first excited singlet state; T_1 : first excited triplet state.

solutions, as shown in Fig. 3. Interestingly, different PL spectral responses are observed when different anions are added. Insignificant changes are detected upon addition of weakly-coordinative Cl^- , Br^- , and non-coordinative ClO_4^- , whereas the addition of F^-

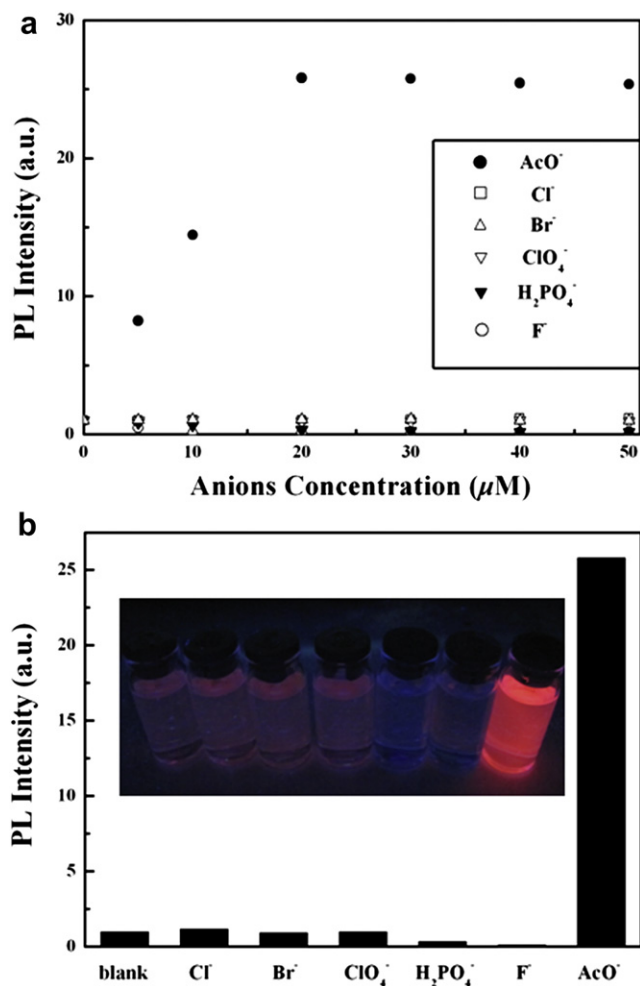


Fig. 3. (a) Normalized PL titrations of $\text{Eu}(\text{DBM})_3\text{DPPZ}$ ($5 \mu\text{M}$) in CH_3CN upon addition of F^- , Cl^- , Br^- , ClO_4^- , H_2PO_4^- , AcO^- . (b) Normalized PL responses of $\text{Eu}(\text{DBM})_3\text{DPPZ}$ in the presence of various anions (Cl^- , Br^- and ClO_4^- : $50 \mu\text{M}$; H_2PO_4^- , F^- , and AcO^- : $20 \mu\text{M}$). Inset: photographs of solutions of the complex in the presence of different anions from left to right in the same sequence as exhibited above, taken under UV illumination. $\lambda_{\text{em}} = 610 \text{ nm}$, $\lambda_{\text{ex}} = 364 \text{ nm}$.

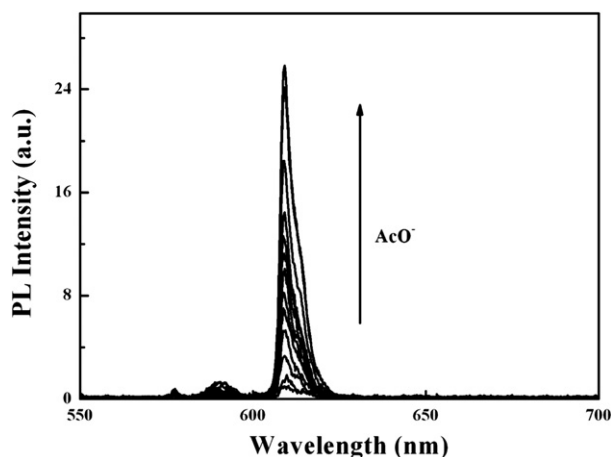


Fig. 4. PL spectra variation of $\text{Eu}(\text{DBM})_3\text{DPPZ}$ ($5 \mu\text{M}$) in the presence of increasing concentration of AcO^- in CH_3CN solution. $\lambda_{\text{ex}} = 364 \text{ nm}$.

and H_2PO_4^- anions decomposes the europium complex, leading to luminescence quenching of the complex. In contrast, the PL intensity sharply increases upon the addition of AcO^- , and this change becomes saturated and exhibits a *ca.* 25.8-fold enhancement when AcO^- reaches about four equivalents of $\text{Eu}(\text{DBM})_3\text{DPPZ}$, which is applicable to naked-eye detection (Fig. 3b). Because of its strong bonding ability, AcO^- is able to substitute DPPZ which is weakly coordinated to Eu^{3+} complex [16], consequently the back-energy transfer from $^5\text{D}_0$ of Eu^{3+} and the triplet state of DBM to the triplet state of DPPZ is restrained. Taken together, these properties render this complex a suitable candidate for the detection of AcO^- with good selectivity.

To further test the recognition ability of $\text{Eu}(\text{DBM})_3\text{DPPZ}$ toward AcO^- , the PL intensity variation of $\text{Eu}(\text{DBM})_3\text{DPPZ}$ ($5 \mu\text{M}$) upon gradual addition of AcO^- ion is monitored under 364 nm excitation. Fig. 4 illustrates the detailed PL spectral response of $\text{Eu}(\text{DBM})_3\text{DPPZ}$ toward AcO^- concentration ranging from 0 to $20 \mu\text{M}$. In the absence of AcO^- , the PL intensity is very weak. Upon increasing concentration of AcO^- , the solution of the complex shows an enhancing luminescence emission at 610 nm (Fig. 4). Meanwhile, the plot of PL intensity of Eu^{3+} emission against the concentration of added AcO^- ion is depicted in Fig. 5. A good linearity between I/I_0 and concentration of AcO^- ion in the range of 0–10 μM is obtained with a linearly dependent coefficient $R^2 = 0.991$. Correspondingly, the

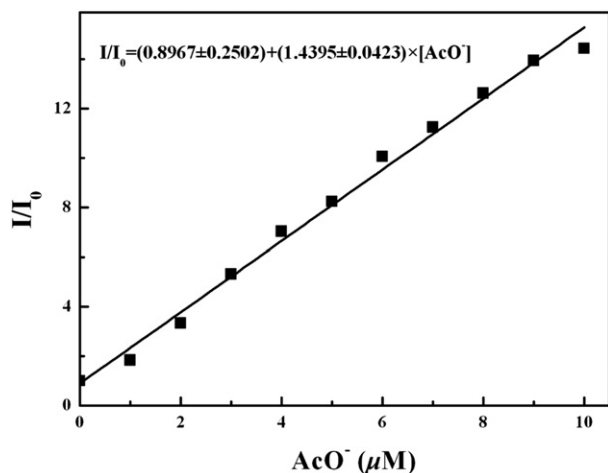


Fig. 5. The plot of normalized PL response I/I_0 of $\text{Eu}(\text{DBM})_3\text{DPPZ}$ ($5 \mu\text{M}$) upon additions of AcO^- from 0 to $10 \mu\text{M}$ in CH_3CN solution. $\lambda_{\text{ex}} = 364 \text{ nm}$.

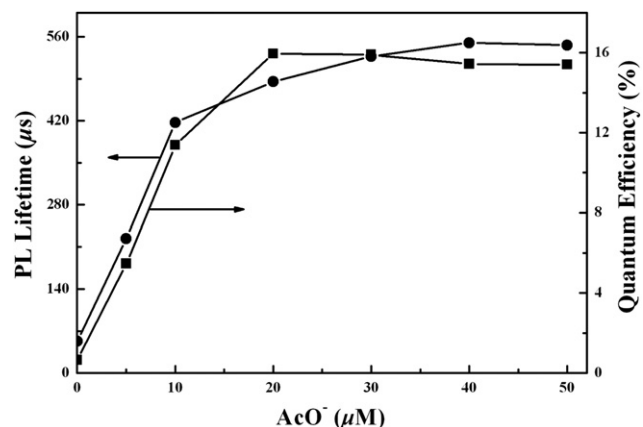


Fig. 6. The plot of PL lifetime and quantum efficiency variations of $\text{Eu}(\text{DBM})_3\text{DPPZ}$ ($5 \mu\text{M}$) in the presence of increasing concentration of AcO^- in CH_3CN solution.

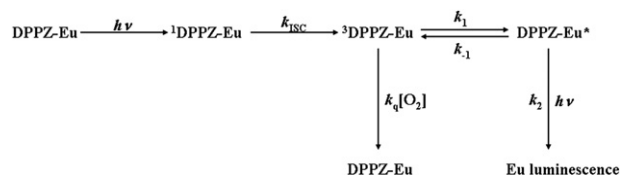
observable sensitivity of the complex is about $1 \mu\text{M}$. Moreover, both the luminescence quantum efficiency and the lifetime of the complex are improved upon gradually addition of AcO^- , which is consistent with the luminescence intensity variation tendency (Fig. 6). Above results indicate that $\text{Eu}(\text{DBM})_3\text{DPPZ}$ possesses high sensitivity for AcO^- and can be used as a luminescent sensor for this anion through naked-eye detection.

3.3. Oxygen sensitivity of $\text{Eu}(\text{DBM})_3\text{DPPZ}$

Generally, the luminescence of most lanthanide complexes is not perturbed by oxygen variations. However, as mentioned above, competitive thermally activated back-energy transfer will occur between the $^5\text{D}_0$ level of the Eu^{3+} ion and the triplet energy of DPPZ ligand. As a consequence, the luminescence of the Eu^{3+} ion becomes sensitive to the presence of oxygen [31]. The mechanism can be tentatively explained by Scheme 2 [20]. Fig. 7 shows the PL spectra of $\text{Eu}(\text{DBM})_3\text{DPPZ}$ in the CH_3CN solution ($5 \mu\text{M}$) under nitrogen, air and oxygen atmospheres. The PL intensity under nitrogen increases *ca.* 4.9-fold compared with that under oxygen. The quantum efficiencies with different dissolved oxygen content are also calculated shown as the inset of Fig. 7 and decreases with enhancement of oxygen content, as consistent with the variation of the PL intensity. On the basis of above results, it can be concluded that $\text{Eu}(\text{DBM})_3\text{DPPZ}$ may be employed for practical applications in the oxygen sensing systems by incorporating the complex into a solid matrix serving as a supporting one which allows oxygen transport from surroundings [20].

3.4. Logic gate express of the luminescence results of $\text{Eu}(\text{DBM})_3\text{DPPZ}$

We have demonstrated that $\text{Eu}(\text{DBM})_3\text{DPPZ}$ could be used in AcO^- sensing and meanwhile, it is sensitive to the presence of oxygen, which enables the europium complex to be fabricated as a more advanced and functional molecular device, such as a logic



Scheme 2. Kinetic scheme of the luminescence of $\text{Eu}(\text{DBM})_3\text{DPPZ}$ quenched by oxygen molecules.

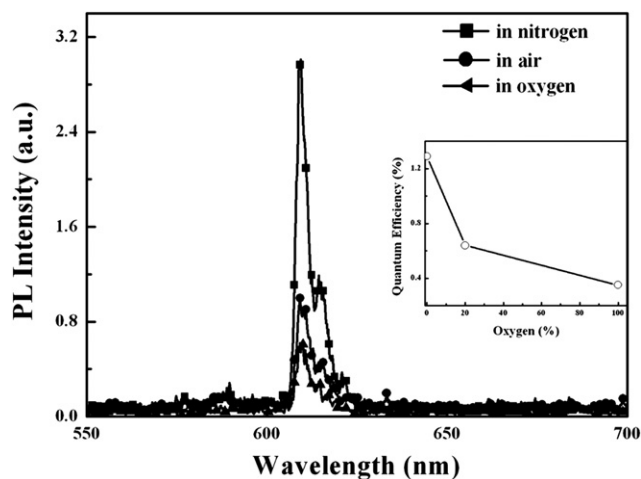


Fig. 7. PL spectra of $\text{Eu}(\text{DBM})_3\text{DPPZ}$ under nitrogen, air, and oxygen in CH_3CN solution ($5 \mu\text{M}$). $\lambda_{\text{ex}} = 364 \text{ nm}$.

gate. Here, the Eu^{3+} emission of $\text{Eu}(\text{DBM})_3\text{DPPZ}$ can be defined as the logic gate output, which provides an entry for developing a molecular logic gate using AcO^- (IN1) and O_2 (IN2) as two inputs. For inputs, the presence and the absence of AcO^- ($2 \mu\text{M}$) and O_2 are defined as 1 and 0, respectively. For output, we define the normalized PL intensity of the complex greater than that under air as 1 (>1) and lower than that under air as 0 (≤ 1). Based on the above definitions, the luminescence decrease of the complex is observed only in the absence of AcO^- under oxygen atmosphere, where the reverse energy transfer occurs, leading to effective luminescence quenching by molecular oxygen, so that the output is read as “0”. Under other circumstances the luminescence of the complex is enhanced, thus leading to output “1”. The PL spectra, the respective symbolic representation of the IMP function and the corresponding truth table are illustrations in Fig. 8. As far as we know, this is the first example of a europium complex logic gate corresponding to a two-input IMP function.

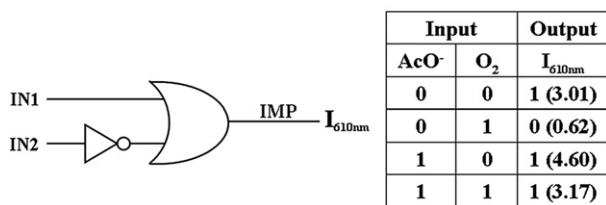
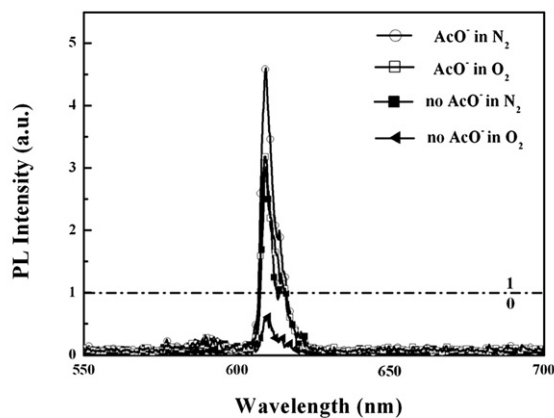


Fig. 8. Top: Normalized PL spectra of $\text{Eu}(\text{DBM})_3\text{DPPZ}$ ($5 \mu\text{M}$) in presence or absence of AcO^- ($2 \mu\text{M}$) with O_2 or N_2 in CH_3CN solution. Bottom: molecular scale implementation and truth table for IMP logic function using the europium complex.

4. Conclusions

In summary, a novel luminescence chemosensor based on a europium complex, $\text{Eu}(\text{DBM})_3\text{DPPZ}$, is designed and synthesized for detection AcO^- in a CH_3CN solution. The europium complex sensor shows a high selectivity for AcO^- ion over other anions and a good linearity between the PL intensity of the complex and the concentration of AcO^- ion, which is applicable to naked-eye detection for AcO^- . The sensing mechanism could be ascribed to the displacement of DPPZ by AcO^- . Moreover, the Eu^{3+} emission is also found to be sensitive to molecular oxygen through a back-energy transfer mechanism. Based on these results, this “off–on”-type luminescence sensor could successfully mimic a molecular level IMP gate with AcO^- and oxygen as the two inputs where the output, a sharp characteristic Eu^{3+} emission, is read as “0” only in the absence AcO^- under oxygen atmosphere. As far as we know, this is the first example of a europium complex logic gate corresponding to a two-input IMP function. We believe that the present system will provide useful information to the range of optical devices that can operate at molecular level.

Acknowledgments

The authors gratefully thank the financial supports of the NSFC (Grant Nos. 51172224 and 51103145) and the Science and Technology Developing Project of Jilin Province (Grant Nos. 20100533 and 201201009).

References

- [1] Bianchi A, Bowman-James K, García-España E. Supramolecular chemistry of anions. New York: Wiley-VCH; 1997.
- [2] de Silva AP, Nimal Gunaratne HQ, Gunnlaugsson T, Huxley AJM, McCoy CP, Rademacher JT, et al. Signaling recognition events with fluorescent sensors and switches. *Chem Rev* 1997;97(16):1515–66.
- [3] Parker D. Luminescent lanthanide sensors for pH, pO_2 and selected anions. *Coord Chem Rev* 2000;205:109–30.
- [4] Martínez-Mañez R, Sancenón F. Fluorogenic and chromogenic chemosensors and reagents for anions. *Chem Rev* 2003;103(11):4419–76.
- [5] Liu ZQ, Shi M, Li FY, Fang Q, Chen ZH, Yi T, et al. Highly selective two-photon chemosensors for fluoride derived from organic boranes. *Org Lett* 2005;7(24):5481–4.
- [6] Han F, Bao YH, Yang ZG, Fyles TM, Zhao JZ, Peng XJ, et al. Simple bithio-carbonohydrazone as sensitive, selective, colorimetric, and switch-on fluorescent chemosensors for fluoride anions. *Chem Eur J* 2007;13(10):2880–92.
- [7] Shao J, Lin H, Lin HK. Rational design of a colorimetric and ratiometric fluorescent chemosensor based on intramolecular charge transfer (ICT). *Talanta* 2008;77(1):273–7.
- [8] Qu Y, Hua JL, Tian H. Colorimetric and ratiometric red fluorescent chemosensor for fluoride ion based on diketopyrrolopyrrole. *Org Lett* 2010;12(15):3320–3.
- [9] Zhu WH, Huang XH, Guo ZQ, Wu XM, Yu HH, Tian H. A novel NIR fluorescent turn-on sensor for the detection of pyrophosphate anion in complete water system. *Chem Commun* 2012;48(12):1784–6.
- [10] Bünzli JCG, Piguet C. Taking advantage of luminescent lanthanide ions. *Chem Soc Rev* 2005;34(12):1048–77.
- [11] Shinoda S, Tsukube H. Luminescent lanthanide complexes as analytical tools in anion sensing, pH indication and protein recognition. *Analyst* 2011;136(3):431–5.
- [12] Pandya S, Yu JH, Parker D. Engineering emissive europium and terbium complexes for molecular imaging and sensing. *Dalton Trans* 2006;25:2757–66.
- [13] Eliseeva SV, Bünzli JCG. Lanthanide luminescence for functional materials and bio-sciences. *Chem Soc Rev* 2010;39(1):189–227.
- [14] Gunnlaugsson T, Leonard JP. Responsive lanthanide luminescent cyclen complexes: from switching/sensing to supramolecular architectures. *Chem Commun* 2005;25:3114–31.
- [15] Charbonnière LJ, Ziessel R, Montalti M, Prodi L, Zaccheroni N, Boehme C, et al. Luminescent lanthanide complexes of a bis-bipyridine-phosphine-oxide ligand as tools for anion detection. *J Am Chem Soc* 2002;124(26):7779–88.
- [16] Zhang DQ, Shi M, Liu ZQ, Li FY, Yi T, Huang CH. Luminescence modulation of a terbium complex with anions and its application as a reagent. *Eur J Inorg Chem* 2006;11:2277–84.
- [17] dos Santos CMG, Fernández PB, Plush SE, Leonard JP, Gunnlaugsson T. Lanthanide luminescent anion sensing: evidence of multiple anion

- recognition through hydrogen bonding and metal ion coordination. *Chem Commun* 2007;32:3389–91.
- [18] Kataoka Y, Paul D, Miyake H, Yaita T, Miyoshi E, Mori H, et al. Experimental and theoretical approaches toward anion-responsive tripod–lanthanide complexes: mixed-donor ligand effects on lanthanide complexation and luminescence sensing profiles. *Chem Eur J* 2008;14(17):5258–66.
- [19] Zhang LM, Li B, Su ZM, Yue SM. Novel rare-earth(III)-based water soluble emitters for Fe(III) detection. *Sensors Actuators B Chem* 2010;143(2):595–9.
- [20] Wang YH, Li B, Zhang LM, Zuo QH, Li P, Zhang J, et al. High-performance oxygen sensors based on Eu(III) complex/polystyrene composite nanofibrous membranes prepared by electrospinning. *ChemPhysChem* 2011;12(2):349–55.
- [21] Zhang XL, Jiao Y, Jing X, Wu HM, He GJ, Duan CY. pH-sensitive fluorescent sensors based on europium(III) complexes. *Dalton Trans* 2011;40(11):2522–7.
- [22] Gunnlaugsson T, Mac Dónail DA, Parker D. Luminescent molecular logic gates: the two-input inhibit (INH) function. *Chem Commun* 2000;1:93–4.
- [23] Bonnet CS, Gunnlaugsson T. Lanthanide macrocyclic quinolyl conjugates as luminescent molecular switches and logic gate functions using HO⁻ and O₂ as inputs. *New J Chem* 2009;33(5):1025–30.
- [24] de Sousa M, de Castro B, Abad S, Mirandab MA, Pischel U. A molecular tool kit for the variable design of logic operations (NOR, INH, EnNOR). *Chem Commun* 2006;(19):2051–3.
- [25] Bo Liang, Zhu MX, Zhu WG. Synthesis and photoluminescence of new europium complex Eu(DBM)₃(DPPZ) with dipyrrophenazine ligand. *Chin Chem Lett* 2003;14(1):43–6.
- [26] Zhang LM, Li B. A series of Eu(III) emitters with a novel triphenylamine-derived beta-diketone ligand. *J Lumin* 2009;129(11):1304–8.
- [27] Zhang LY, Li B, Zhang LM, Chen P, Liu SY. Synthesis, characterization, and luminescent properties of europium complexes with fluorine functionalized phenanthroline. *J Electrochem Soc* 2009;156(3):H202–7.
- [28] van der Tol EB, van Ramesdonk HJ, Verhoeven JW, Steemers FJ, Kerver EG, Verboom W, et al. Tetraazatriphenylenes as extremely efficient antenna chromophores for luminescent lanthanide ions. *Chem Eur J* 1998;4(11):2315–23.
- [29] Steemers FJ, Verboom W, Reinhoudt DN, van der Tol EB, Verhoeven JW. New sensitizer-modified calix[4]arenes enabling near-UV excitation of complexed luminescent lanthanide ions. *J Am Chem Soc* 1995;117(37):9408–14.
- [30] Zhang LM, Li B, Zhang LY, Su ZM. Reduced efficiency roll-off in organic light-emitting diodes by a novel short-lived organoeuropium emitter. *ACS Appl Mater Interfaces* 2009;1(9):1852–5.
- [31] Parker D, Senanayake PK, Williams JAG. Luminescent sensors for pH, pO₂, halide and hydroxide ions using phenanthridine as a photosensitizer in macrocyclic europium and terbium complexes. *J Chem Soc Perkin Trans* 1998;2(10):2129–39.